

tron irradiations.<sup>11</sup> It is also of interest to compare the photoneutron displacement effects with those produced by high-energy electron irradiations. Irradiation of silicon with 30-MeV electrons is expected to produce recoils with an average energy of 180 eV, leading to approximately 4.5 displaced atoms per primary collision, compared with an average of  $\sim 5000$  for the  $(\gamma, n)$  recoils. Hence, the defect cluster produced will be much smaller than those produced in the  $(\gamma, n)$  experiments and fast-neutron irradiations.

The rate of change of reciprocal lifetime for 30-MeV electrons has been measured to be  $d(1/\tau)/d\phi = 4.5 \times 10^{-8}$  cm<sup>2</sup>/sec. The calculated rate of introduction of displaced atoms is

$$dN_a/d\phi = 17 \text{ cm}^{-1}.$$

Therefore, the rate of change of lifetime per displaced atom, without considering annealing, is

$$d(1/\tau)/dN_a = 2.6 \times 10^{-9} \text{ cm}^3/\text{sec}.$$

This value is smaller by a factor of more than 20 than even the highest energy  $(\gamma, n)$  results (see Table I) and becomes even smaller when compared to the lower energy  $(\gamma, n)$  results. A similar result is obtained upon comparison of the result for the change in reciprocal Hall coefficient  $1/R_H$ , which measures the rate of acceptor introduction in *n*-type silicon. This observation is similar to the results of Wertheim<sup>11</sup> who concluded

<sup>11</sup> G. K. Wertheim, Phys. Rev. **111**, 1500 (1958).

that neutrons produce localized damage regions containing a large number of recombination centers.

## VI. SUMMARY

The production of displacement radiation effects by photoneutron recoils has been established by measuring the relative rates of defect production in silicon by various energy bremsstrahlung spectra. The change in the reciprocal of the lifetime is approximately proportional to the total number of primary reactions, with a proportionality constant of  $(2.0 \times 10^4 \pm 25\%) \text{ cm}^3 \text{ sec}^{-1}$ . The data can be explained on the basis that the primary energy-loss mechanism is due to ionization. Similar experiments in germanium should establish the validity of this conclusion.

Another interesting result is that the rate of change of reciprocal lifetime and reciprocal Hall coefficient are found to be about an order of magnitude smaller for high-energy electron irradiations. No explanation of this result is possible at this time, but is probably caused by a high density of recombination centers being formed by the photoneutron reactions.

## ACKNOWLEDGMENTS

The authors wish to acknowledge gratefully the valuable assistance of J. W. Harry and H. Horiye in conducting the experiments, D. K. Nichols in the associated theoretical calculations, and S. K. Boehm and C. M. Faulkner in the data reduction.

## Characteristic *K*-Shell X-Ray Production in Magnesium, Aluminum, and Copper by 60- to 500-keV Protons\*

J. M. KHAN AND D. L. POTTER

*Lawrence Radiation Laboratory, University of California, Livermore, California*

(Received 12 September 1963)

Characteristic *K*-shell x rays produced when protons of 60- to 500-keV energy are stopped in thick targets of magnesium, aluminum, and copper have been studied using a proportional counter of conventional design. The thick target yields were measured. The x-ray production cross sections have been calculated for the *K* shells. Ionization cross sections have been estimated and were found to be smaller than the values predicted by the Born approximation in all cases.

### INTRODUCTION

CHARACTERISTIC x rays produced when charged particles pass through matter were detected as early as 1913.<sup>1</sup> Early experiments, in studying the energy losses suffered by heavy, high-speed ions, attempted to determine average atomic ionization cross sections and also average atomic ionization potentials. Another approach is to measure separately the ionization cross sections of the various atomic shells. The

conventional method involves detection of the radiation emitted following an ionizing event. (This number must, however, be corrected for the radiationless reorganization of the atom.)

When the bombarding ions (protons in the case considered here) are of low energy they may lose all of their energy in even the thinnest self-supporting target. Under these "thick" target conditions the x-ray yield is measured. From this thick target yield it is possible to obtain the x-ray production cross section. When corrected for the fluorescent yield of the shell, this then gives the ionization cross section,

\* This work was performed under the auspices of the U. S. Atomic Energy Commission.

<sup>1</sup> J. Chadwick, Phil. Mag. **25**, 193 (1913).

The first absolute  $K$ -shell yield measurement was made in 1936 by Peter (for 132-keV protons on aluminum).<sup>2</sup> The number obtained approximates the thick target yield measured here. Since then many experiments have been performed using higher energy ions to produce characteristic x rays of energies greater than 2 keV.<sup>3,4</sup>

The present work extends the measurements down to proton energies of 60 keV and to characteristic x-ray quantum energies of 1.3 keV. Aluminum and copper were selected for the first measurements performed using the newly constructed target chamber shown in Fig. 1. This choice of characteristic x rays allows comparison with previous experiments employing other methods: the absolute  $K$ -shell yield in aluminum at 132 keV (Peter<sup>2</sup>) and the thick target yield measurements in the  $K$  shell of copper under bombardment of protons of energies 150 to 500 keV (Messelt<sup>5</sup>). The measurements agree within 15%.

The estimated ionization cross sections are compared with theoretical calculations based on the Born approximation. It is found that in all cases the measured values are smaller than predicted. The cross section for the  $K$  shell in copper as obtained by both Messelt and the authors is in good agreement with values predicted by a semiclassical treatment in which deflection of the bombarding particle by the Coulomb field of the nucleus is also considered.<sup>6</sup>

#### EXPERIMENTAL APPARATUS AND METHODS

The main components of the experimental equipment are (1) a proton source, (2) magnetic analyzer, (3) beam collimator, (4) secondary electron shield, (5) target holder, (6) absorption foil changer, (7) flow-mode (P-10 gas) proportional counter, (8) amplifiers, (9) differential discriminator and scalar, and (10) pulse-height analyzer [400 channel (RIDL) in coincidence with output of discriminator]. This list follows the order of encounter (1) of the proton from source to target, (2) of the x ray from target to counter, and (3) pulse from counter to scalar and analyzer.

The proton source and magnetic analyzer are components of the Cockcroft-Walton accelerator at the Lawrence Radiation Laboratory, Livermore, California. The accelerator has the capability of producing protons having a continuous energy range from 60 to 500 keV. Beam currents between 0.1 and 5  $\mu$ A were employed. In the present experiment two independent

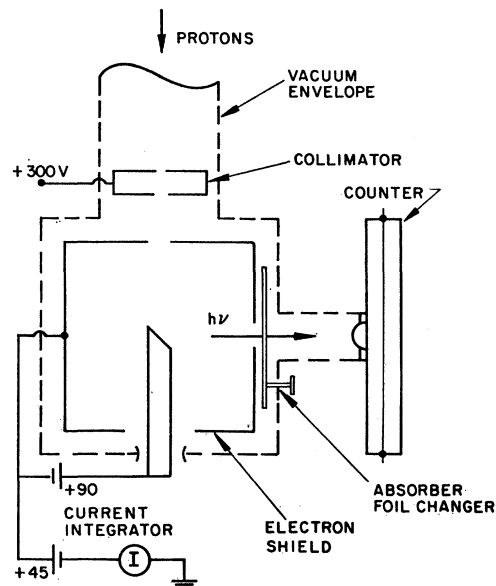


FIG. 1. Target chamber.

methods were used to calibrate the energy of the beam. The low-energy region (less than 150 keV) was calibrated by the use of a precision resistor string. At higher energies three resonances in a LiF target were employed.

A comment should be made regarding the calibration method. The potential drop suffered by the accelerated protons is monitored by a resistor string voltage divider. The total resistance from the base of the quartz tube of the ion source to ground is 2400 M $\Omega$ . The resistor string employs 2100 M $\Omega$  of resistance external (and immersed in oil) to the Cockcroft-Walton shell which contains the initial focusing structure. Inside the shell there is an additional 300 M $\Omega$ . During the course of preliminary measurements it was found that at voltages greater than 300 kV, the 300-M $\Omega$  internal resistance would not appear in the voltage divider resistance. It was felt that corona from the shell jumped to the top of the 2100-M $\Omega$  external resistor (see point "A," Fig. 2) raising it to the potential of the shell, hence producing a reference voltage from the string that was higher than the correct value by the ratio 2400/2100.

After solving the problems of corona shorting of the resistor string and establishing the linearity of the voltage divider, a second effect was found. It was observed that the resonance peaks appeared at a voltage higher than expected (by as much as 40 keV for the LiF targets studies). Previous experimenters<sup>4</sup> at this Laboratory employed the "thin" target resonances at 340, 441, and 483 keV in LiF to calibrate the reference voltage resistor string, mistakenly identifying the peak with the reported resonance energy. Thick (>0.4 mg/cm<sup>2</sup>) LiF targets were then employed, with the resonance energy identified with the point of maximum slope of the side of the resulting quasistep function. These points were found to be internally consistent and agreed to within  $\pm 1\%$  of the values predicted by the lower voltage calibration of the resistor string.

<sup>2</sup> O. Peter, Ann. Physik 27, 299 (1936). In the present experiment the proton enters the target at 45° and likewise the detected radiations emerge at the same angle—both traveling an equal distance in the target material. In the experiment of Peter, the protons enter normal to the surface, with the detected radiation emerging from the opposite face of the target foil. This method requires assumptions as to the range of the protons in the target.

<sup>3</sup> Review of field—E. Merzbacher and H. W. Lewis, *Encyclopedia of Physics* (Springer-Verlag, Berlin, 1958), Vol. 34, p. 166.

<sup>4</sup> R. C. Jopson, H. Mark, and C. D. Swift, Phys. Rev. 127, 1612 (1962).

<sup>5</sup> S. Messelt, Nucl. Phys. 5, 435 (1958).

<sup>6</sup> J. Bang and J. M. Hansteen, Kgl. Danske Videnskab. Selskab, Mat.-Fys. Medd. 31, No. 13 (1959).

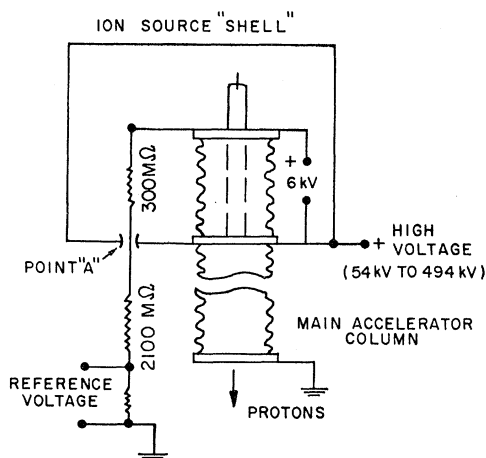


FIG. 2. Cockcroft-Walton high-voltage system.

The beam collimator consisted of two disks separated by  $\frac{3}{8}$  in. The hole in the disk on the source side was  $\frac{1}{4}$  in. in diameter, while that on the target side was  $\frac{3}{8}$  in. These two disks were held at a positive voltage of 300 V relative to ground. It has been found that a number of electrons (as much as 10% of the beam in the worst cases) pass down the beam pipe with the protons. These were produced by glancing collisions of imperfectly focused protons with the walls. Secondary electrons in great abundance were also produced at the edge of the collimating disks. A positive voltage of over 50 V relative to ground on the two disks was found to greatly reduce the contribution of electrons from these two sources, and 300-V positive voltage to give an electron-to-proton ratio of less than 0.1%.

The target holder and secondary electron shield were connected together to form a charge collecting unit. The target holder was biased 90 V positive with respect to the shield, and the shield 45 V positive with respect to ground (through a current integrator). By measuring the currents flowing in the various legs of the system (with and without the target holder in place) the following observations were made: (1) less than 1% of the proton beam struck the outside of the shield, (2) a 10% electron flow from the shield to the target assembly occurred—attributable, presumably, to photoelectron ejection from the shield by low-energy quanta produced in the target ( $E \leq 100$  eV), and subsequent attraction to the positively biased target. (This observation leads us to be somewhat skeptical of the standard suppressor plate technique used to retain secondary electrons on targets in a close geometry.<sup>7</sup>)

An absorption foil changer was employed to establish the transmission of the proportional counter window. Two samples of the window material stock were used—one in the counter and one in the foil changer. There was an observable distortion (bowing) of the 0.00040-in. aluminum counter window produced by the atmospheric pressure difference across the  $\frac{1}{2}$ -in.-diam window. Therefore a distorted window was also mounted in the foil

changer. The increased transmission of the distorted window for x rays of energy greater than 2 keV was less than 1%, but for the Al *K* radiation was 7%, and for the Mg *K* radiation was 15%.

The proportional counter employed was of conventional design—2 in. in diameter, 12 in. long, and with a center wire of 0.003-in.-diam stainless steel. The counting gas (*P*-10) is 90% argon, 10% methane, used at atmospheric pressure in a flow mode at 100 cc/min. The voltage on the center wire is +2150 V. For the Al and Mg *K* radiation the gas in the counter represented over 10 absorption lengths. For the 8.1-keV Cu *K* radiation only 64% of the radiation was stopped within the counter. Identification of the lines was made simple by calibration with an Fe<sup>55</sup> source giving a 6-keV Mn *K* line. The counter has been shown to have a peak pulse height with is proportional to the quantum energy to  $\pm 3\%$  over the range from 284 eV to 12 keV. The counter had a background count rate of 50 counts/min, where the usual signals were over 1000 counts/min. One eccentricity was observed. When a Mylar window (0.00013 in.) was used there were many irregularly shaped pulses seen (which were observed only during bombardment of the target) of continuous distribution up to heights corresponding to 10-keV x rays. One possible explanation might involve collection of electrons on the nonconducting Mylar surface, with subsequent breakdown. (Space applications of Mylar window proportional counters may have similar problems.)

The complete target chamber is shown in Fig. 1. The distance between the target holder and counter window was altered by a factor of 2 to test the validity of the point source assumption in calculating the solid angle factor. The yields measured at these two distances agreed to within 2%.

In discussing the experimental method, the state of

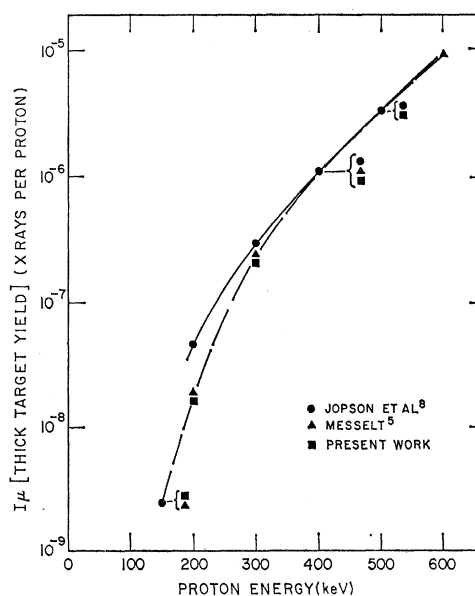


FIG. 3. Copper thick target yield.

<sup>7</sup> B. Singh, Phys. Rev. **107**, 711 (1957).

TABLE I. Thick target yield table.

Element	Z	$E_p$ (keV)	$N(E)$ (x rays per $\mu$ C before geometrical and absorption corrections)	$I_\mu^a$ ( $\pm 15\%$ ) (x rays per proton)	$I_\mu$ (previous measurements)	$dI_\mu/dE$ (x rays per proton per keV)
Magnesium	12	60	81	$2.40 \times 10^{-7}$		$1.90 \times 10^{-8}$
		100	1 120	$3.31 \times 10^{-6}$		$1.55 \times 10^{-7}$
		150	7 580	$2.24 \times 10^{-5}$		$7.17 \times 10^{-7}$
		200	27 500	$8.13 \times 10^{-5}$		$1.85 \times 10^{-6}$
		300	162 000	$4.79 \times 10^{-4}$		$6.90 \times 10^{-6}$
		400	486 000	$1.44 \times 10^{-3}$		$1.33 \times 10^{-5}$
		500	1 040 000	$3.07 \times 10^{-3}$		$1.66 \times 10^{-5}$
$\frac{\Lambda}{A} = \frac{3364}{(0.182)_w}$						
Aluminum	13	60	70	$1.05 \times 10^{-7}$		$8.63 \times 10^{-9}$
		100	994	$1.52 \times 10^{-6}$		$7.78 \times 10^{-8}$
		132	3 880	$5.90 \times 10^{-6}$	$6.22 \times 10^{-6b}$	$2.19 \times 10^{-7}$
		150	7 100	$1.08 \times 10^{-5}$		$3.27 \times 10^{-7}$
		200	27 200	$4.14 \times 10^{-5}$		$9.63 \times 10^{-7}$
		300	170 000	$2.58 \times 10^{-4}$		$3.83 \times 10^{-6}$
		400	551 000	$8.39 \times 10^{-4}$		$8.55 \times 10^{-6}$
500	1 250 000	$2.07 \times 10^{-3}$		$1.72 \times 10^{-5}$		
$\frac{\Lambda}{A} = \frac{3364}{(0.33)_w}$						
Copper	29	150	2.41	$2.31 \times 10^{-9}$	$2.5 \times 10^{-9c}$	$1.24 \times 10^{-10}$
		200	18.0	$1.73 \times 10^{-8}$	$1.9 \times 10^{-8c}$	$5.46 \times 10^{-10}$
		300	218	$2.09 \times 10^{-7}$	$2.4 \times 10^{-7c}$	$4.08 \times 10^{-9}$
		400	1 127	$1.08 \times 10^{-6}$	$1.17 \times 10^{-6c}$	$1.55 \times 10^{-8}$
		500	3 600	$3.45 \times 10^{-6}$	$3.5 \times 10^{-6c}$	$3.39 \times 10^{-8}$
$\frac{\Lambda}{A} = \frac{3364}{(0.874)_w (0.643)_c}$						

<sup>a</sup>  $I_\mu = N(E) \cdot (\Lambda/A_{w,c})$ , where  $\Lambda$  is the geometrical factor and  $A$  is the window ( $w$ ) and counter gas ( $c$ ) absorption correction factor.  
<sup>b</sup> See Ref. 2.  
<sup>c</sup> See Ref. 5.

the target surface can not be neglected at a low x-ray quantum energy (less than 3 keV) or a low proton energy (less than 200 keV). Two conditions were found to effect the x-ray yields measured. The first was the roughness of the surface after the initial cleaning (effecting the self-absorption path lengths for the x rays). The second was the surface contamination which took place during bombardment (this appeared to have the effect of reducing, somewhat, the energy of the protons in the energy region where the stopping power of the decomposed pump oils is high, i.e., less than 200 keV).

The following cleaning procedures were employed: (1) sanding surface with 600-grit paper, (2) mirror surface polishing (metal polish), and (3) chemical etching. The first two procedures were followed by thorough washing in water-free ethanol. The first procedure gave thick target yields, which were a function of the angle between the sanding direction and plane containing the proton beam and detector, having a maximum value at 0° and minimum (25% below maximum for  $h\nu \approx 1$  keV) value at 90°. The second procedure yielded results equivalent with the maximum values for the first procedure. The third method produced yields which were below those of the first two procedures by about 7%. These variations are only seen for x-ray energies less than 3 keV, and are independent of proton energy.

The second effect is that of surface contamination during bombardment. The beam pipe leading to the target chamber is kept at  $5 \times 10^{-5}$  mm Hg while the target chamber itself is kept at  $1 \times 10^{-6}$  mm Hg by a separate, trapped (liquid-nitrogen) oil diffusion pump. For 60-keV protons at a current of 30  $\mu$ A the yield was observed to drop 7% in 5 min and at 100 keV, 3% in

5 min. The drop is most correlatable with the product  $I_p \cdot t$  (proton current  $\times$  time), rather than time from cleaning, time in air prior to placement in vacuum system, or time in vacuum system prior to bombardment. Each of these times was varied by a factor of 10 with no observable effect.

MEASUREMENTS

The x-ray production cross section can be computed from the thick target yield by using the formula

$$\sigma_x(E) = \frac{1}{n} \left( \frac{dI_\mu}{dE} \right) [S(E)] + \frac{1}{n} \bar{\mu} I_\mu$$

The ionization cross section is given by

$$\sigma_I(E) = (1/\bar{\omega}) \sigma_x$$

where  $\bar{\omega}$  is the fluorescent yield appropriate to the shell and levels involved. In the above expression,  $\sigma_x(E)$  is the x-ray production cross section in  $\text{cm}^2$ ,  $n$  is the number of target atoms per milligram,  $dI_\mu/dE$  is the slope of the thick target yield function in number of x rays per incident proton per keV,  $S(E)$  is the stopping power in  $(\text{keV cm}^2/\text{mg})$ ,  $I_\mu(E)$  is the number of x rays observed per incident proton at energy  $E$ , and  $\bar{\mu}$  is the mass absorption coefficient of the target material for its own characteristic radiations.

Tables I and II summarize the yield and cross section results. When possible the yield values are compared with the results of other experimenters. This occurs at 132 keV in aluminum, where the agreement is within 6%. In the copper K shell, the values are compared with the 1958 results of Messelt and are found to agree

TABLE II. Ionization cross-section table.

Element	Z	$E_p$ (keV)	$S(E)^d$ (keV-cm <sup>2</sup> /mg)	$\sigma_x$ (x-ray production-cm <sup>2</sup> )	$\bar{\omega}_K$	$\sigma_I$ (exptl) (ionization-cm <sup>2</sup> )	$\sigma_I$ (theoret) (ionization-cm <sup>2</sup> )	$\frac{\sigma_I(\text{theoret})}{\sigma_I(\text{exptl})}$
Magnesium $\frac{\bar{\mu}^a}{\rho} = 441 \frac{\text{cm}^2}{\text{g}}$	12	60	425	$3.5 \times 10^{-25}$	0.021	$1.7 \times 10^{-23}$	$2.43 \times 10^{-22}$	14
		100	430	$2.8 \times 10^{-24}$		$1.3 \times 10^{-22}$	$1.01 \times 10^{-21}$	7.7
		150	385	$1.2 \times 10^{-23}$		$5.5 \times 10^{-22}$	$2.63 \times 10^{-21}$	4.7
		200	350	$2.8 \times 10^{-23}$		$1.3 \times 10^{-21}$	$4.69 \times 10^{-21}$	3.6
		300	306	$9.4 \times 10^{-23}$		$4.5 \times 10^{-21}$	$0.95 \times 10^{-20}$	2.1
		400	280	$1.8 \times 10^{-22}$		$8.4 \times 10^{-21}$	$1.40 \times 10^{-20}$	1.66
500	260	$2.3 \times 10^{-22}$		$1.1 \times 10^{-20}$	$1.81 \times 10^{-20}$	1.65		
Aluminum $\frac{\bar{\mu}^b}{\rho} = 390 \frac{\text{cm}^2}{\text{g}}$	13	60	434	$1.7 \times 10^{-25}$	0.029	$5.9 \times 10^{-24}$	$1 \times 10^{-22}$	17
		100	414	$1.5 \times 10^{-24}$		$5.2 \times 10^{-23}$	$4.6 \times 10^{-22}$	8.9
		132	385	$3.9 \times 10^{-24}$		$1.3 \times 10^{-22}$	$9.9 \times 10^{-22}$	7.6
		150	370	$5.6 \times 10^{-24}$		$1.9 \times 10^{-22}$	$1.2 \times 10^{-21}$	6.3
		200	337	$1.5 \times 10^{-23}$		$5.2 \times 10^{-22}$	$2.3 \times 10^{-21}$	4.4
		300	292	$5.5 \times 10^{-23}$		$1.9 \times 10^{-21}$	$4.7 \times 10^{-21}$	2.5
		400	267	$1.2 \times 10^{-22}$		$4.1 \times 10^{-21}$	$7.8 \times 10^{-21}$	1.9
500	249	$2.3 \times 10^{-22}$		$7.9 \times 10^{-21}$	$1.0 \times 10^{-20}$	1.3		
Copper $\frac{\bar{\mu}^c}{\rho} = 50.9 \frac{\text{cm}^2}{\text{g}}$	29	150	225	$3.0 \times 10^{-27}$	0.39	$7.5 \times 10^{-27}$	$1 \times 10^{-25}$	13
		200	220	$1.3 \times 10^{-26}$		$3.3 \times 10^{-26}$	$3.3 \times 10^{-25}$	10
		300	202	$8.8 \times 10^{-26}$		$2.2 \times 10^{-25}$	$1.3 \times 10^{-24}$	5.9
		400	184	$3.1 \times 10^{-25}$		$7.8 \times 10^{-25}$	$3.3 \times 10^{-24}$	4.2
		500	170	$6.3 \times 10^{-25}$		$1.6 \times 10^{-24}$	$6.4 \times 10^{-24}$	4

<sup>a</sup> B. L. Henke, R. White, B. Lundberg, J. Appl. Phys. **28**, 98 (1957).

<sup>b</sup> A. J. Bearden, Ph. D. thesis, Johns Hopkins University, 1958 (unpublished).

<sup>c</sup> *Handbook of Chemistry and Physics* (Chemical Rubber Publishing Company, Cleveland, 1958), 42nd ed.

<sup>d</sup> S. D. Warshaw, S. K. Allison, Rev. Mod. Phys. **25**, 779 (1953).

to within 15%. In addition, the results of Jopson *et al.*,<sup>8</sup> Messelt,<sup>5</sup> and the present work are plotted in Fig. 3. It has been established that the two sources of error in energy calibration previously discussed were present in the experiments of Ref. 4.<sup>9</sup> Although it is not possible to determine the correct energies at this point, the limits of error in energy are large enough to allow agreement with the results of Messelt and this work. The cross sections for the copper *K* shell are within 15% of the values of Messelt, using the same values for  $\mu$ ,  $S(E)$ , and  $\bar{\omega}_K$ .

Also tabulated in Table II are the values of  $\sigma_I$  as calculated from the Born approximation as presented by Merzbacher and Lewis.<sup>3</sup> The exact calculation was made based upon the work of Walske.<sup>10</sup>

#### DISCUSSION AND CONCLUSION

As can be seen from Table II, the Born approximation calculation predicts ionization cross sections which are higher than those observed by an amount which in-

<sup>8</sup> R. C. Jopson, H. Mark and C. D. Swift (private communication).

<sup>9</sup> In Ref. 4, the data are presented in two parts. First are the yields and cross sections at the energy identified with 441 keV. The second are relative measurements from 200 to 500 keV normalized to the "441" results. Re-evaluating the data of Ref. 4, the following is apparent: The energy identified with 441 keV was  $454 \pm 10$  keV; the resonance misassignment and corona-induced reference voltage nonlinearity suggest an energy assignment at 200 keV lower than the correct energy by as much as 30 keV.

<sup>10</sup> M. C. Walske, Phys. Rev. **101**, 940 (1956).

creases rapidly as the bombarding proton energy decreases. This is to be expected if the Bang and Hansteen analysis is correct—that is, the increased Coulomb deflection of the projectile by the nuclear charge as the bombarding energy decreases, hence increasingly deviating from the plane-wave calculation.<sup>6</sup> The above calculation for the Cu *K* shell shows a marked improvement over the plane-wave predictions. It therefore seems most desirable to extend this calculation to the *K* shells of lower *Z* materials and to include *L* and *M* shells where possible.

The agreement of the yields of the current experiment with those of Messelt and Peter suggests that the proportional counter method is well suited to the measuring of thick target yields in the energy range less than 10-keV quantum energy. The problems encountered in the measurement of even the thick target yields are substantial, as can be seen reflected in the spread in the results obtained in the previous years.<sup>3,4,7</sup> The two most serious problems are energy calibrations (reflected in the steep slope of the yield curves) and the accurate measurement of the bombarding ion current.

#### ACKNOWLEDGMENTS

The authors would like to express their thanks to Dr. H. Mark and Dr. R. C. Jopson and C. D. Swift for their help and suggestions, and to R. Cedarlund, F. Stoutamore, and B. Beliz for their assistance in operating the Cockcroft-Walton accelerator.